SPECTRAL CHARACTERISATION OF LAND SURFACE COMPOSITION TO DETERMINE SOIL EROSION WITHIN SEMIARID RAINFED CULTIVATED AREAS

Thomas Schmid[1], Alicia Palacios-Orueta[2], Sabine Chabrillat[3], Eyal Bendor[4], Antonio Plaza[5], Manuel Rodriguez[1], Margarita Huesca[2], Marta Pelayo[1], Cristina Pascual[2], Paula Escribano[6], Victor Cicuendez[2]

[1]CIEMAT, Avda. Complutense 40, 28040 Madrid, Spain. thomas.schmid@ciemat.es
[2] Departamento de Silvopascicultura, E.T.S.I Montes, UPM. 28040 Madrid, Spain.
[3]GFZ German Research Centre For Geosciences, Telegrafenberg, 14473 Potsdam, Germany.
[4]Department of Geography and Human Environment, Tel Aviv University, Israel.
[5]Hyperspectral Computing Laboratory, University of Extremadura, E-10071 Cáceres, Spain.
[6]Department of Soil Science and Agrochemistry, University of Almería, E-04120 Almería, Spain.

ABSTRACT

In a Mediterranean semiarid area in Central Spain, with dominant rainfed agriculture, hyperspectral airborne data, supported by field spectroscopy have been obtained, allowing a spectral identification of bare soil with the corresponding erosion stages. The definition of soil erosion stages is based on a spectral characterization supported by morphological, physical and chemical features of contrasted soil surfaces as a result of soil loss. Different soil erosion stages were defined within two bare-soil sites representing the soil variability of the area, and where such stages are spatially represented. The validation of selected image derived endmebers was a key step to carry out a partial unmixing for determining soil erosion stages. A preliminary spatial distribution of advanced and intermediate erosion stages was obtained for the most representative soil types.

Index Terms— Soil erosion, hyperspectral data, unmixing, semiarid, rainfed agriculture

1. INTRODUCTION

Soils within Mediterranean areas form part of a fragile ecosystem, but are greatly influenced by extensive human activities that imply an agricultural land use affecting soil conditions. Factors such as climate, crop rotation, agricultural practices and policy regulations have a profound impact on the management of cultivated lands. In these areas, plant cover and land uses are considered the most important factors explaining the intensity of soil erosion [1, 2]. Soil erosion, as a consequence of tillage, represents a major factor of transformation in soil landscapes (mixture and inversion of horizons; soil truncation; substitution of horizons) within Mediterranean environments [3]. Spatial distribution patterns of eroded soils on slopes under agricultural use can only be explained as an accumulated effect of tillage practices overlapped by hydrological and wind erosion processes [3].

In flat cultivated areas, tillage occurring in alternate directions for consecutive years produces a random movement of the soil material with no defined direction over the terrain. However, in areas even on gentle slopes the resulting soil movement is not the same in all directions. There is a close relation between soil movement and slope. Ploughing with a tractor up slope will not compensate the loss of soil originated from the same work when moving down slope. Thus, in this type of landscape even when there is no significant development of rills or gullies, this process generates a net loss of soil [3, 4] that frequently is not evident.

The main aim of this work is to identify and characterize soil erosion stages applying high resolution remote sensing data for gently sloping agricultural areas within Central Spain. This includes: 1) establishing the corresponding soil erosion stages for the selected areas, 2) implementing field spectroscopy and airborne hyperspectral data for identifying soil surface characteristics related to erosion; and 3) and applying spectral unmixing techniques to determine spatial distribution of the soil erosion stages.

2. STUDY AREA

The study area (*Figure 1*) is located in the centre of Spain, in the north-west sector of the Autonomous Community of Castilla-La Mancha, Province of Toledo, approximately 50 km SW from Madrid. Common characteristics such as Mediterranean climate, extended agricultural rain-fed uses, mostly evolved soils, and erosion features associated to contrasting soil horizons are representative for areas in Southern Europe.

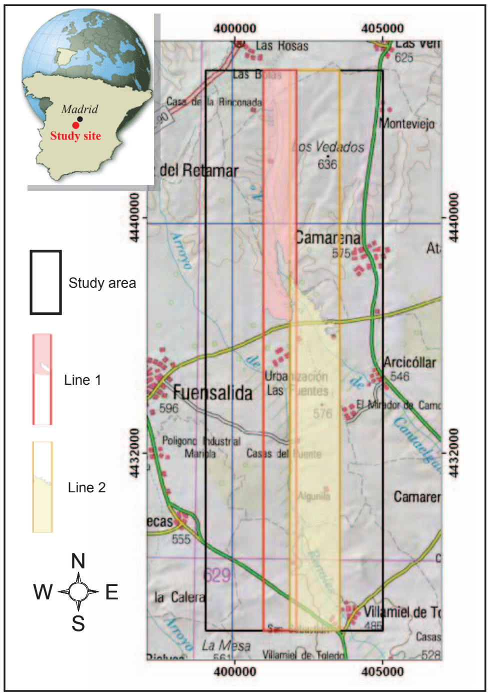

Figure 1. Study area of Camarena delimited by two flight lines (1 and 2) from the 2011 EUFAR flight campaign and within the corresponding shaded areas.

The study area is approximately 114 km^2 and is situated in the Tagus Basin (South Iberian Meseta), and corresponds to the Guadarrama river catchment. The climate is Mediterranean, with a continental variant that shows cool winter temperatures, and low precipitations with maximum in late autumn, winter and late spring and an outstanding minimum in summer. The average monthly temperature is in the range of 6.1 to 24.7ºC with an average annual temperature of 14.6ºC and an average monthly rainfall of 7 to 56 mm with an average yearly rainfall of 429 mm, respectively. An important variability is observed between different years. Such variability is eventually related to erosive events.

The substrate is formed by Miocene arkoses (feldspars, quartz and phyllosilicates as main constituents and locally calcite), and Quaternary associated sediments constituting forms as glacis, terraces and alluvial fans. Such materials and forms are associated to a gently undulating relief, at altitudes between 500 and 640 m a.s.l. Dominant soils are: Alfisols and Inceptisols (Xeralfs and Xerepts, according to the Soil Taxonomy [5]), or Luvisols and Calcisols (IUSS Working Group WRB, 2006). The typical profile is characterized by an A horizon, a Bt horizon and a C horizon that overlies the arkose. A typical Xerept profile is characterized by an A horizon that directly overlies a Ck horizon resulting from altered limestone. Erosion intensity and ploughing practices determine the presence of different soil surface horizons with these contrasting soil properties.

3. METHODOLOGY

The methodological procedure is presented in *Table 2*.

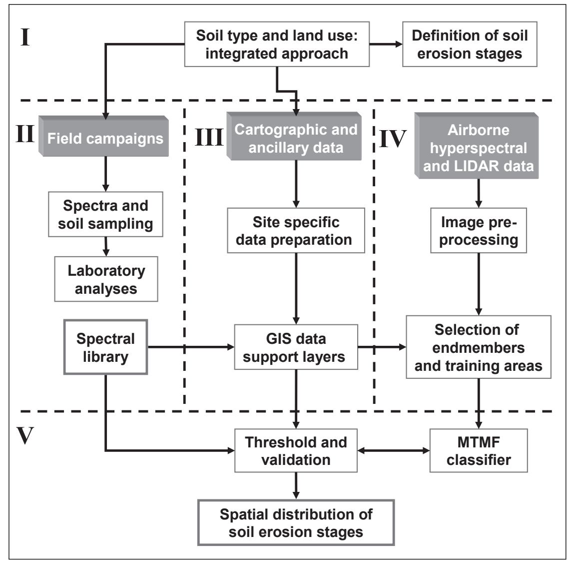

Figure 2. Methodological procedure.

A first part established the relation between soil type and land use for defining soil erosion stages within a selected study area. As a first approach, two sites within the study area (E1 to the North and SU to the South within the shaded areas of line 1 and 2 in *Figure 1*) were selected with an extension of 10 ha each; such plots correspond to bare soils, recently submitted to ploughing, and they are representative of main soil types of the study area. The plots contain well developed soils formed on arkose, limestone (carbonated layer within the arkose), and quaternary sediments within a gently sloping topography.

Part II was aimed at obtaining data during field campaigns in 2011 which coincided with data acquisitions described below. Portable spectroradiometers (ASD FieldSpec3 and ASD Pro) within the spectral range of 350 to 2500 nm were used to obtain different soil surface covers. Soil samples were collected, prepared, and physical and chemical laboratory analyses included soil colour, texture, free iron oxide content, organic matter (OM) content and mineralogy. A spectral library was compiled with field spectra and soil analyses to obtain key reference spectra of characteristic surface conditions associated to soil erosion and for identifying and verifying results.

A further part was dedicated to cartographic and ancillary data (topography, lithology, geomorphology and land use). A Geographic Information System (GIS) was used to manage and compile a georeferenced database of all the generated data of this work. This enables GIS techniques to be applied to the georeferenced data to create support layers.

Part IV processed the hyperspectral airborne AISA Eagle and Hawk data and ALS50 (II) airborne laser scanner

(LIDAR) data that were acquired on the 8th of August 2011 through a grant from the European Facility For Airborne Research (EUFAR). This was simultaneously carried out with the corresponding field campaign obtaining field spectral data and soil samples supported by the Spanish National R&D program. A pre-processing of the hyperspectral AISA Eagle and Hawk data includes radiometric, geometric and atmospheric correction. A high resolution digital terrain model of the study area was created from the LIDAR data for the pre-processing steps of the hyperspectral data and to provide detailed topographic information for determining erosion and land cover conditions. A further step was the selection of endmembers and training areas to represent the different soil erosion stages. In this case, image processing included the minimum noise fraction (MNF) [6]. The corresponding components were input to the pixel purity index (PPI) procedure [7] to determine spectrally the most pure pixels within the dataset. The MNF and PPI results were then projected into an n-dimensional visualizer to determine image-derived endmembers. A pool of endmembers representing the different soil erosion stages as well as related land use surfaces was created. Identification and labelling of the endmembers was carried out comparing key field spectra and verifying the location in the field.

In part III, the selected image-derived endmembers corresponding to the different soil erosion stages were introduced into the mixed tuned match filtering (MTMF), a partial unmixing algorithm (Boardman, 1998). To obtain the most accurate classification of each endmember, a 2-D scatter plot of matched filter (MF) values versus infeasibility was plotted. Pixels identified with a high MF and low infeasibility were considered to have the purest endmember pixels. Optimum threshold values were determined comparing the spectral profile of matched pixels against the endmember spectral profile.

4. RESULTS AND DISCUSSION

The soils in the study area show contrasting horizons, in terms of physical, chemical and mineralogical properties (*Table 1*). As a result of erosion processes, different horizons emerge at the soil surface showing a clear contrast of exposed soil properties. Furthermore, areas of accumulation must be considered, where mixed materials corresponding to eroded soil horizons are deposited. The main horizons present in the study area include A horizons with a low OM content; fine textured Bt horizons and C or Ck (rich in calcite) horizons. As a result, the presence of surfaces with properties related to A, Bt or C/Ck horizons at the surface is used to define different stages of increasing erosion, as well as mixed materials within the accumulation areas. Thus, the northern site (Xeralfs on coarse arkoses) shows surface materials as C horizon within eroded summits (point E1-P1: advanced stage of erosion, losing A and B horizons), as Bt horizons on middle slopes (points E1-P2 and E1_P3: middle stage of erosion, losing Ap horizon), and as Ap horizons as a result of accumulation of mixed soil material on lower or bottom slopes (point E1-P4: stage of accumulation). On the other hand, the southern site (Xerepts and Xeralfs on fine arkoses, locally limestones) shows surface material as carbonated Ck horizons on eroded summits (points SU-2, SU-5 and SU-6: advanced stage of erosion within Xerepts, losing A horizon), as Bt horizons on middle slopes (points SU-1 and SU-3: middle stage of erosion in Xeralfs, losing the Ap horizon), and as Ap horizons constituted by sandy arkosic material on lower or bottom slopes (point SU-4: stage of accumulation).

Table 1. Soil properties for the test sites E1 and SU.

PARAMETERS		*NORTH AREA (COARSE ARKOSE)*				*SOUTH AREA (FINE ARKOSE)*					
		E1-P1	E1-P2	E1-P3	E1-P4	SU1	SU2	SU3	SU4	SU5	SU6
pH (H_2O 1:2.5)		5.69	5.88	5.62	5.54	7.80	8.22	7.80	5.24	8.46	8.28
E.C. (1:5; $\mu S*cm^{-1}$)		42.3	47.2	64.8	29.4	152.6	173.5	145.4	100.6	186.5	192.1
O.M. (% w/w)		0.5	0.5	0.9	0.2	0.8	1.1	0.5	0.5	0.5	1.0
Fe_2O_3 (% w/w)		0.12	0.54	0.36	0.23	0.43	0.08	0.17	0.17	0.22	0.25
Mineralogy (semiquantitative %)	Qrz	59	40	38	48	48	21	50	52	24	14
	K-Fd	32	28	12	34	6	9	16	29	7	6
	Plg	5	3	3	8	6	15	8	12	9	6
	Phy	4	29	46	10	36	13	27	7	54	33
	Cal	0	0	0	0	5	42	0	0	7	40
C. F. (% >2mm)		11.1	9.4	9.4	8.4	1.4	36.2	14.8	1.7	1.6	3.3
Texture (% <2 mm)	clay	7.8	40.3	27.8	5,3	32.8	20.3	21.4	7.8	27.8	37.8
	silt	6.7	5.7	9.7	10,2	18.7	23.7	10.1	14.2	38.7	26.2
	sand	85.5	54.0	62.5	84.5	48.5	56.0	68.5	78.0	33.5	36.0
Munsell Soil Color (dry)	hue	10YR	7.5 ; 5YR	10YR	10YR	7,5YR	10YR	10YR	10YR	10YR	10YR
	value	7	5 - 4	5	6	5	7,5	5	7	6.5	7
	chroma	3	4 - 5	3	3	3	2	2.5	3	3	2.5

E.C.: *Electrical conductivity*
O.M.: *Organic matter.*
Mineralogy: Qrz: *Quartz;* K-Fd: *K-Feldspars;* Plg: *Plagioclase;* Phy: *Phyllosilicates;* Cal: *Calcite.*
C.F: *Coarse fragments*

The presence at the surface of contrasting soil properties, described above, is consequently the result of erosion processes. The term “soil erosion stage”, in this study, is defined as a qualitative term and is based on studies [3, 4] focused on tillage-induced soil erosion. These stages were then implemented as a spatial model for determining their distribution within the selected sites E1 and SU.

Initial results show that spectral analyses (*Figure* 3) of the emerging soil horizons are key to the successful interpretation of the main soil erosion stages. Spectral differences are mainly related to variations in the overall spectral brightness that is strongly influenced by the texture, organic matter, iron oxide, calcium carbonate content and the mineral composition. These differences are particularly observed between stable and eroded soil surfaces in different hill slope position (summit, shoulder or back slope). Areas of accumulation are more difficult to differentiate as they are influenced by the type and kind of mixing of the eroded material as well as slope gradient and shape. In this case, the digital terrain model is used to further improve the spatial definition between the stable, eroded and accumulated areas.

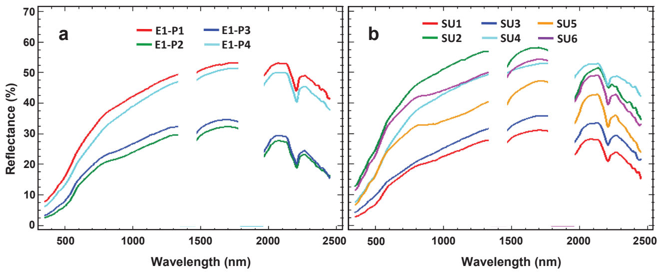

Figure 3. Field spectra of the different soil horizons for a) site E1 and b) site SU.

Figure 3 shows the spectral characteristics of different soil erosion stages that are both present in the northern and southern sites respectively. E1-P1 shows advanced erosion and E1-P2 and E1-P3 are areas with an intermediate erosion stage. The same applies for SU2 and SU1 where the erosion stage is advanced and intermediate respectively.

The spectral analyses lead to a careful selection of field-derived endmembers that are implemented in the MTMF unmixing classifier using the hyperspectral data (*Figure 4*).

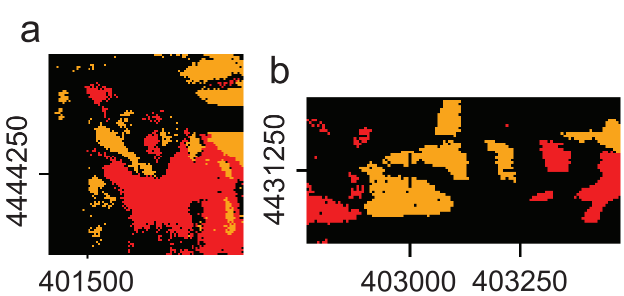

Figure 4. Spatial distribution of the advanced (red) and intermediate (orange) erosion stages in a) E1 and b) site SU.

This includes a spectral identification of different bare soils in which erosion stages are defined. The advantage of this approach is to integrate the field information and unmixing techniques to determine the most representative erosion stages where unmixing can model the sub-pixel composition by means of abundance estimation techniques. Applying thresholds that were determined with the reference spectra, preliminary results show that the classifications and the spatial distributions within the studied test plots were well determined. A further important aspect of the spectral analyses is shown in the scaling issue of between different sensor data. Through this method, a significant improvement of determining the soil erosion stages is expected when the spatial resolution changes between future hyperspectral sensor acquisitions. Furthermore, ongoing work includes integrating the traditional classification assigning hard labels to describe the most representative erosion stages while unmixing can model the sub-pixel composition by means of abundance estimation techniques [9], thus combining both techniques in synergistic fashion in the hyperspectral data interpretation.

5 ACKNOWLEDGEMENTS

The authors would like to sincerely thank the Airborne Research and Survey Facility of the Natural Environment Research Council (ARSF NERC) flight operators and the ARSF Data Analysis Node Remote Sensing group for the efficient management of the hyperspectral and lídar data acquisition and pre-processing, respectively. Many thanks go to Ms. Ashley Bracken at GFZ for pre-processing of the Hyperspectral data. The authors acknowledge funding of the data by the European Fleet for Airborne Research (EUFAR) and support from the Spanish Science R&D program with the project AGL2010-17505.

6. REFERENCES

[1] C. Kosmas, N. Danalatos, L.H. Cammeraat, M. Chabart, J. Diamantopoulos, R. Farand, L. Gutiérrez, A. Jacob, H. Marques, J. Martínez-Fernández, A. Mizara, N. Moutakas, J.M. Nicolau, C. Oliveros, G. Pinna, R. Puddu, J Puigdefábregas, M. Roxo, A. Simao, G. Stamou, N. Tomasi, D. Usai and A. Vacca, "The effect of land use on runoff and soil erosion rates under Mediterranean conditions," *Catena*, vol. 29, pp. 45–59, 1997.

[2] J.M. García-Ruiz, "The effects of land uses on soil erosion in Spain: A review," *Catena*, vol. 81, pp. 1–11, 2010.

[3] S. De Alba, "Modeling the effects of complex topography and patterns of tillage on soil translocation by tillage with mouldboard plough," *Journal of Soil and Water Conservation*, vol. 56, pp. 335-345, 2001.

[4] M.J. Lindstrom, W.W. Nelson, and T.E. Schuhmacher, "Quantifying tillage erosion rates due to moldboard plowing," *Soil & Tillage Research*, vol. 24, pp. 243-255, 1992.

[5] Soil Survey Staff, "Keys to Soil Taxonomy", 11th ed. USDA-Natural Resources Conservation Service, Washington, DC., 2010.

[6] A.A. Green, M. Berman, P. Switzer and M. D. Craig, "A transformation for ordering multispectral data in terms of image quality with implications for noise removal," *IEEE Transactions on Geoscience and Remote Sensing*, vol. 26, No. 1, pp. 65-74, Jan. 1988.

[7] J.W. Boardman, F.A. Kruse and R.O. Green, "Mapping target signatures via partial unmixing of AVIRIS data," in Summaries of the Fifth JPL Airborne Earth Science Workshop, JPL Publication 95-1(1), pp. 23-26.

[8] J.W. Boardman, Leveraging the high dimensionality of AVIRIS data for improved sub-pixel target unmixing and rejection of false positives: Mixture tuned matched filtering. Summaries of the Seventh JPL Airborne Geoscience Workshop. JPL Publication 97-1, pp. 55–56, 1998.

[9] I. Dopido, M. Zortea, A. Villa, A. Plaza and P. Gamba, "Unmixing prior to supervised classification of remotely sensed hyperspectral images," *IEEE Geoscience and Remote Sensing Letters*, vol. 8, no. 4, pp. 760-764, 2011.